W. PIEKARSKA*, M. KUBIAK*, Z. SATERNUS*, K. REK*

# COMPUTER MODELLING OF THERMOMECHANICAL PHENOMENA IN PIPES WELDED USING A LASER BEAM

# KOMPUTEROWE MODELOWANIE ZJAWISK TERMOMECHANICZNYCH W RURACH SPAWANYCH Z WYKORZYSTANIEM WIĄZKI LASEROWEJ

This study concerns numerical modelling and computer simulation of thermomechanical phenomena accompanying spiral welding of pipes made of stainless steel X5CrNi18-10 using a laser beam. Based on Abaqus FEA software, 3D numerical analysis was performed. Power distribution of spirally moving heat source was implemented into additional DFLUX subroutine, written in Fortran programming language. Thermomechanical properties of steel changing with temperature were taken into account in the analysis. The efficiency of material melting by different welding sources as well as the influence of heat load on the shape of melted zone, deformation of welded pipe and residual stress were examined.

*Keywords*: Laser welding, hybrid welding, numerical modelling, helical seam pipe

Praca dotyczy modelowania numerycznego i symulacji komputerowej zjawisk termomechanicznych towarzyszących procesowi spawania spiralnego rur ze stali nierdzewnej X5CrNi18-10 przy wykorzystaniu wiązki laserowej. Bazując na oprogramowaniu Abaqus FEA wykonano analizę numeryczną 3D. Rozkład mocy źródła ciepła poruszającego się spiralnie implementowano w dodatkowej procedurze DFLUX napisanej w języku programowania Fortran. W analizie uwzględniono zmienne własności termomechaniczne stali. Badano efektywność przetapiania materiału różnymi typami źródeł spawających oraz wpływ obciążenia cieplnego na kształt strefy przetopienia, deformacje spawanych rur i naprężenia spawalnicze.

## 1. Introduction

Manufacturing of spirally welded pipes proceeds in fully automated production lines where hot strip is shaped into a tube by spiral forming with a constant bending radius. Helically formed material is then automatically welded inline by continuously joining abutting strip edges [1-3], usually using gas metal arc welding (GMAW) or gas tungsten arc welding (GTAW) methods. Among the worldwide applications of helical seam pipes, they are mainly used in gas or fluid transmission pipelines [2]. Typical applications include pumping stations, wastewater treatment, chemical processing, storm water down-pipes, ventilation ducts, etc [3].

In recent years, laser welding technology is becoming one of the leading modern manufacturing techniques. Constantly developed new welding equipment and the possibility of full automation of the process open up new possibilities for laser welding technique in the industry [4, 5]. This joining method has also much less thermal impact on the material. In laser welding high transmission speed is achieved while maintaining required properties of the weld. In comparison with conventional techniques [6]. Therefore, laser welding is most efficient for thin plate applications. The advantages of laser welding, including good quality of welds with obtained a significant reduction of welding distortion, result in increased efficiency and flexibility of pipelines production at lower operating costs.

Recently hybrid welding, combining laser welding with classic electric arc welding is under particular investigations. The use of two heat sources cooperating in a single process allows obtaining proper joint with simultaneously reduced energy costs and increased welding speed [7, 8]. This welding technique allows for greater tolerances in fit-up in contrast to single laser beam welding and smaller welding distortion in comparison to classic arc welding.

During welding temperature field generates thermal strain, in consequence residual stress as the elastoplastic response of the object towards the transient thermal stresses. It is generally know that welding stress can be a major source of cracking and fracture in welded structures. Therefore, accurate prediction of stresses induced by the welding process can be extremely helpful in the design of welded constructions. The rapid development in computer sciences allows analyzing difficult, coupled thermomechanical phenomena as well as predicting distortion and stress in welded pipes.

Very important in terms of formal modelling of mechanical phenomena accompanying heat transfer in steel is a proper description of heat energy distribution in the material taking into account the real process conditions as well as a proper theoretical approach with temporary and residual stress taken

* CZĘSTOCHOWA UNIVERSITY OF TECHNOLOGY, INSTITUTE OF MECHANICS AND MACHINE DESIGN FOUNDATIONS, DĄBROWSKIEGO 73, 42-200 CZĘSTOCHOWA, POLAND

into considerations that have a great influence on mechanical properties of the material [9, 10]. The effect of metal heating during welding, in consequence distortion and welding stress, mostly depends on the amount and distribution of heat load. In numerical modelling of welding processes using a laser beam a different approach is required in terms of process theory, because heat distribution proceeds in different conditions in comparison to classic welding techniques. Material is rapidly heated to high temperatures reaching or even exceeding the boiling point of steel [10, 11]. Moreover, the amount and distribution of heat load in hybrid welding depend on two coupled heat sources of different types: electric arc and laser beam [11, 12].

Changes in material state during welding require appropriate description of solid-liquid transformation in theoretical considerations. Temperature field during material melting and solidification is affected by the latent heat of fusion. Macro models describing solidification process for both pure metals [13-15] and alloys [16-18] can be found in the literature. Mostly, one domain approach is used with effective heat capacity [16] that can be easily discretized and numerically solved.

This work presents a three-dimensional finite element modelling of thermal and mechanical phenomena in spirally welded pipes. Numerical analysis is performed in Abaqus FEA commercial software completed by additional DFLUX subroutine used to implement the distribution and helical motion of welding sources. Three different models describing laser beam, electric arc and laser-arc hybrid heat sources are used in calculations in order to analyze the influence of heat load and process parameters on the deformation and residual stress of spirally welded pipes.
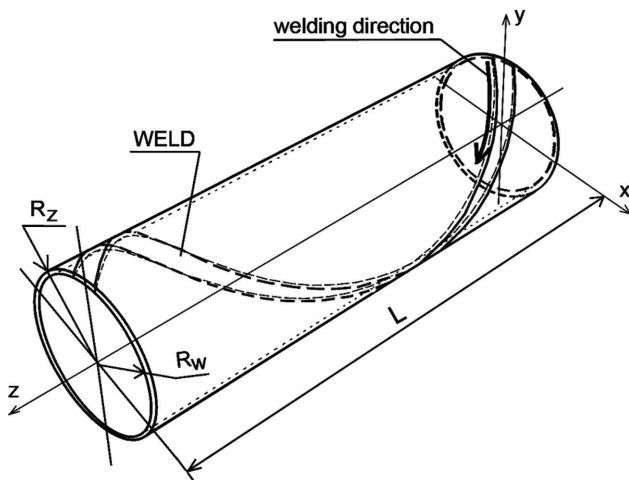


Fig. 1. Scheme of considered system

## 2. Numerical modelling

Numerical simulations were executed in Abaqus FEA assuming thermal and mechanical analysis in separate two steps (Fig. 2) [19, 20]. Thermal analysis is performed as "Uncoupled heat transfer" task. Results obtained during the first step of analysis are used in mechanical analysis executed as „Static General" task where isotropic strain generated by temperature distribution is considered for every simulation time period.
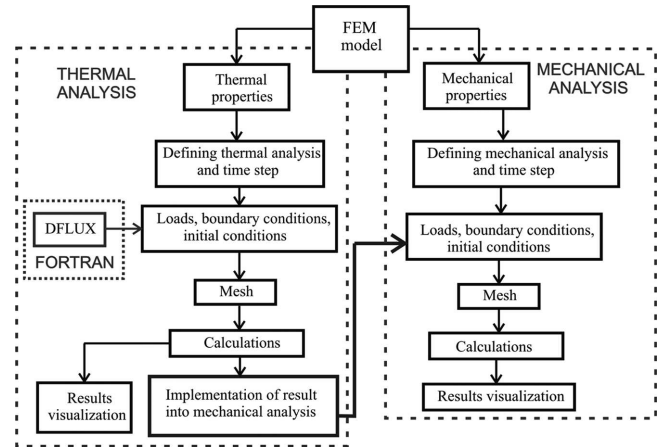


Fig. 2. Diagram of thermomechanical analysis performed in Abaqus FEA

Three dimensional finite element model was developed for spirally welded pipe with dimensions $R_z$ =30 mm, $R_w$ =28.4 mm, $L$ =200 mm (Fig. 1). Figure 3 shows finite element mesh used in calculations. Both analysis steps use the same cuboid finite element mesh with the highest density in the helical welding line. It is assumed that element dimension perpendicular to welding line increases along distance from the center of movable heat source. Finite element mesh used in calculations consists of 44409 elements.
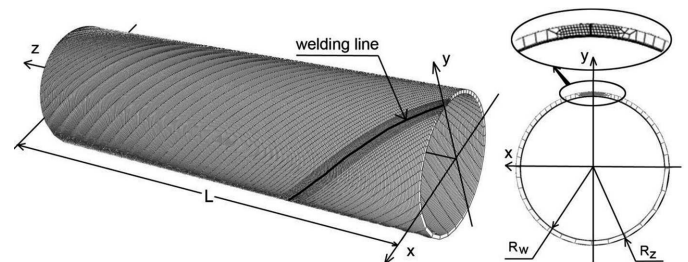


Fig. 3. Finite element mesh used in numerical analysis

### 2.1. Movable heat source models

Gaussian model is used with linear decrease of energy density along material penetration depth to describe distribution of a laser beam power [21]:

$$q_v(r, z) = \frac{Q_L}{\pi r_o^2 s} \exp\left[\left(1 - \frac{r^2}{r_o^2}\right)\right]\left(1 - \frac{z}{s}\right) \qquad (1)$$

where $Q_L$ is laser beam power [W], $r_0$ is beam radius [m], $r$ is actual radius [m], $s$ is penetration depth [m], $z$ is actual penetration [m].

Widely accepted by the researchers, defined by Goldak [22] 'double ellipsoidal' power distribution of a heat source is used to simulate arc welding conditions. This heat source consists of two half-ellipsoids expressed as follows:

$$q_v = \begin{cases} q_1(x,y,z) = \dfrac{6\sqrt{3}f_1 Q_A}{abc_1\pi\sqrt{\pi}} \times \exp(-3\dfrac{x^2}{c_1^2}) \times \exp(-3\dfrac{y^2}{a^2}) \times \\ \qquad\qquad \exp(-3\dfrac{z^2}{b^2}) \quad \text{for } x < x_o \\ q_2(x,y,z) = \dfrac{6\sqrt{3}f_2 Q_A}{abc_2\pi\sqrt{\pi}} \times \exp(-3\dfrac{x^2}{c_2^2}) \times \exp(-3\dfrac{y^2}{a^2}) \times \\ \qquad\qquad \exp(-3\dfrac{z^2}{b^2}) \quad \text{for } x \geqslant x_o \end{cases}$$

(2)

where $a, b$, $c_1$ and $c_2$ are set of axes defining front ellipsoid and rear ellipsoid, $f_1$ and $f_2$ ($f_1 + f_2 = 2$) represent distribution of the source energy at the front and the rear section of the source, thus resultant distribution of the source energy is total sum described as $q_v(x,y,z) = q_1(x,y,z) + q_2(x,y,z)$ and $Q_A$ is the arc heat source power.

Gaussian distribution (1) and Goldak model (2) are used in computer simulation of laser-arc hybrid welding process. In this case heat sources cooperating in tandem along welding line. Relative arrangement with leading electric arc is assumed and with the distance between heat sources $d = 3$ mm.

Heat source models are implemented into DFLUX subroutine with defined spiral movement along surface of a pipe. The motion of heat source in Cartesian coordinates system is expressed as follows:

$$\begin{cases} x = R_Z \sin(\varphi_0 + \omega \cdot t) \\ y = R_Z \cos(\varphi_0 + \omega \cdot t) \\ z = z_0 + v_2 \cdot t \end{cases}$$

(3)

where $R_z$ is outer radius of the pipe [m], $t$ is time [s], $\varphi_0$ is the angle of the initial position of heat source on the outer shell, $\omega = v_1 \cdot t$ is angular speed in which $v_1 = $const is peripheral speed, $z_0$ is a initial position on the axis $z$, $v_2$ is an axial speed along $z$ axis. Welding speed $v$ is the result of the peripheral $v_1$ and axial $v_2$ speed $v = \sqrt{v_1 + v_2}$, as presented in Fig. 4.
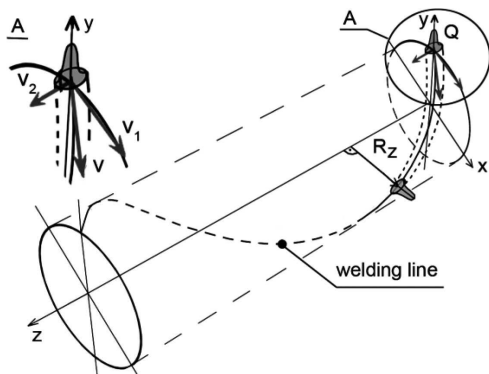


Fig. 4. Scheme of spiral heat source movement

## 2.2. Thermal and mechanical analysis

Energy conservation equation and Fourier's law are numerically solved in Abaqus FEA to determine temperature field in welded pipe. Governing equation in thermal analysis is completed by initial condition and boundary conditions of Dirichlet, Neumann and Newton type with heat loss due to convection, radiation and evaporation taken into considerations. The variational formulation of energy conservation equation is expressed as follows:

$$\int_V \rho \dot{U} \delta T \, dV + \int_V \frac{\partial \delta T}{\partial x_\alpha} \cdot \left( \lambda \frac{\partial T}{\partial x_\alpha} \right) dV = \int_V \delta T \, q_V dV + \int_S \delta T \, q_S dS$$

(4)

where $\lambda = \lambda(T)$ is a thermal conductivity [W/(m K)], $U$ is a internal energy, $q_v$ is laser beam heat source [W/m$^3$], $q_S$ is a heat flux toward element surface [W/m$^2$], $\delta T$ is a variational function, $\rho$ is density [kg/m$^3$].

Latent heat associated with solid-liquid transformation ($H_L = 260 \times 10^3$ J/kg) is taken into account in specific heat $c(T) = dU / dT$ [J/(kg K)], assuming linear approximation of solid fraction between solidus and liquidus temperatures ($T_S = 1400°$C and $T_L = 1455°$C).

Obtained thermal history is used in mechanical analysis of spirally welded pipe. The equilibrium equation and constitutive relations are expressed in the rate form:

$$\nabla \circ \dot{\sigma}(x_\alpha, t) = 0, \qquad \dot{\sigma}_{ij} = \dot{\sigma}_{ji}$$
$$\dot{\sigma} = \mathbf{D} \circ \dot{\varepsilon}^e + \dot{\mathbf{D}} \circ \varepsilon^e, \quad \varepsilon = \varepsilon^e + \varepsilon^p + \varepsilon^{Th}$$

(5)

where $\sigma = \sigma(\sigma_{ij})$ is stress tensor, $x_\alpha$ describes location of considered point (material particle), ($\circ$) is inner exhaustive product, $\mathbf{D} = \mathbf{D}(T)$ is a tensor of temperature dependent material properties, $\varepsilon$ is total strain, $\varepsilon^\mathbf{e}$ is elastic strain, $\varepsilon^\mathbf{p}$ is plastic strain and $\varepsilon^{\mathbf{Th}}$ is thermal strain.

Equation (5) is completed by boundary conditions specified to prevent rigid body motion and initial conditions: $\sigma(x_\alpha, t_0) = \sigma(x_\alpha, T_S) = 0$, $\varepsilon(x_\alpha, t_0) = \varepsilon(x_\alpha, T_S) = 0$.

After assuming perfect plasticity of material and strain-rate independent with isotropic strain-hardening, plastic deformation obeys the von Mises criterion. Considering temperature dependent material properties and yield strength as well as plastic flow model with plastic deformation obeying von Mises criterion, strain rate can be expressed in the following form:

$$\dot{\varepsilon}_{ij} = \frac{1}{2G}\dot{S}_{ij} - \frac{1}{2G^2}\dot{G}S_{ij} + \frac{1-\nu}{E}\dot{\sigma}\delta_{ij} - \frac{1-2\nu}{E^2}\dot{E}\sigma_m\delta_{ij} -$$
$$- \frac{2}{E}\dot{\nu}\sigma_m\delta_{ij} + \dot{\varepsilon}^{Th}\delta_{ij} + \frac{3S_{ij}}{2\bar{\sigma}H'}\dot{\bar{\sigma}} + \frac{3S_{ij}}{2\bar{\sigma}H'}\frac{\partial f}{\partial T}\dot{T}$$

(6)

where $E = E(T)$ is Young's modulus, $G = G(T)$ is the shear modulus and $\upsilon$ is Poisson's ratio, $\sigma_m$ denotes the mean stress, $\delta_{ij}$ is the Kronecker delta. Cauchy stress tensor $\sigma_{ij} = S_{ij} + \sigma_m\delta_{ij}$ can be derived by an inverse relation of Eq. (6).

Thermal and mechanical properties of X5CrNi18-10 stainless steel with chemical composition: 0.06 C, 17-19 Cr, 11-13 Ni and N<0.11 [%] are presented in Fig. 5 [23].
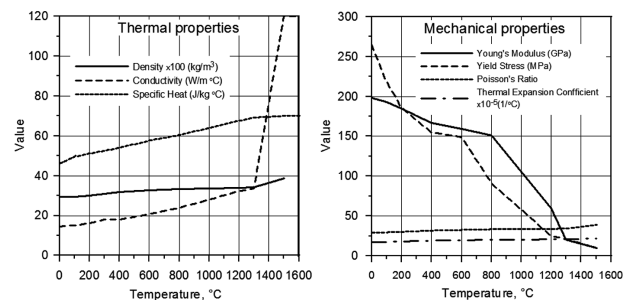


Fig. 5. Thermomechanical properties assumed in calculations

## 3. Results and discussion

Computer simulations were performed for three different models of heat sources describing power distribution of a laser beam, laser-arc hybrid welding sources and (as a comparison) classic electric arc welding source. Obtained results allowed the assessment of analyzed welding method and process parameters in terms of joint quality and mechanical properties of spirally welded pipes. The effects of thermal load on the weld pool shape, welding distortion and residual stress was compared for performed welding simulations. The laser beam heat source parameters were set basing on the experimental research made in [24], while for other analyzed processes-to ensure full material penetration with similar thermal influence zone. Heat sources parameters are summarized in Table 1.

TABLE 1

Heat sources parameters assumed in calculations

| Heat sources parameters | Laser beam welding, Eq. (1) | Arc welding, Eq. (2) | Laser-arc welding |
|---|---|---|---|
| Power | $Q_L = 1000$ W | $Q_A = 1000$ W | $Q_A = 300$ W, $Q_L = 600$ W |
| Geometry | $r_0 = 0.9$ mm, $s = 2$ mm, | $c_1 = 2$ mm, $c_2 = 5$ mm, a= 1.5 mm, $b = 0.5$ mm, $f_1 = 0.6$, $f_2 = 1.4$ | Sources offset: $d = 3$mm *Arc:* $c_1 = 2$ mm, $c_2 = 5$ mm, $a = 1.5$ mm, $b = 0.5$ mm, $f_1 = 0.6$, $f_2 = 1.4$ *Laser:* $r_o = 0.9$ mm, $s = 2$ mm |
| Welding speed | $v = 30$ mm/s | v= 25 mm/s | $v = 40$ mm/s, |

### 3.1. Temperature field

Figures 6-8 show a three-dimensional temperature profile for specified process time with marked melted zone boundary ($T_L \approx 1455°C$), at the outer and inner surfaces of the pipe welded by laser beam (Fig. 6), electric arc (Fig. 7) and hybrid method (Fig. 8). On the basis of obtained results it can be stated that laser welding provided narrow melted zone (width of the weld is 2.7 mm at the outer surface and 1.4 mm at the inner surface of the pipe) in comparison to arc welding.

In order to ensure full material penetration during electric arc welding, heat source speed was reduced. As a result of material melting by the electric arc heat source wider melted zone is obtained (about 2 mm at the outer surface and 2.5 mm at the inner surface of the pipe).

Due to the interaction of both heat sources in the welding pool during hybrid welding process lower heat source power and higher welding speed are sufficient for complete material penetration with retained melted zone shape similar to this obtained in the simulation of single laser beam welding (Fig. 6 and Fig. 8).
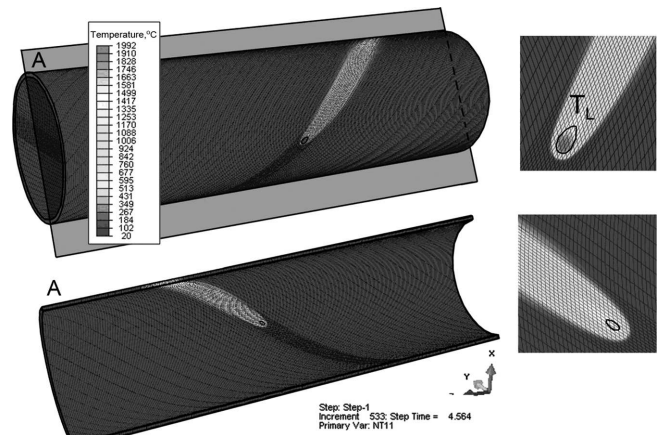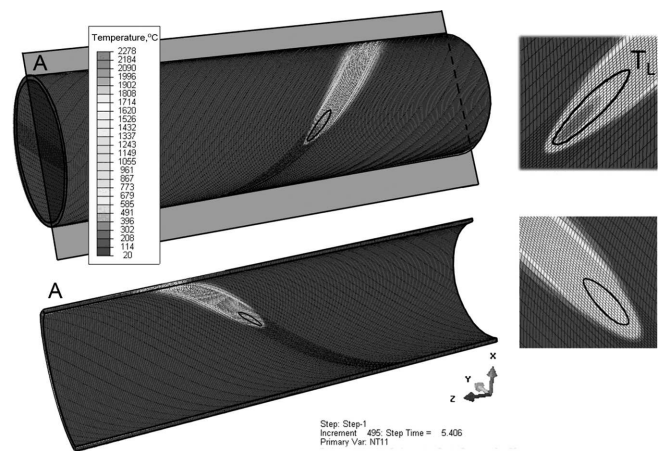


Fig. 6. Temperature profile of laser welded pipe


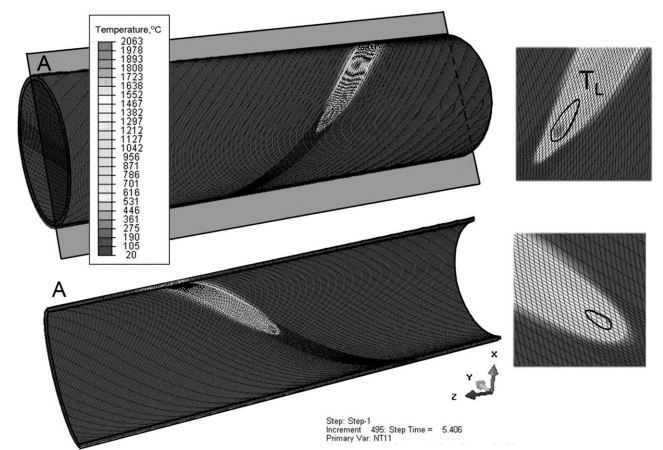
Fig. 7. Temperature profile of electric arc welded pipe



Fig. 8. Temperature profile of laser-arc hybrid welded pipe

### 3.2. Distortion and stress

Figure 9 shows overall distortion of spirally welded pipe after laser welding (Fig. 9a), arc welding (Fig. 9b) and hybrid welding (Fig. 9c) respectively with marked vectors (directions) of deformation. It can be observed that largest distortion appears at both ends of the pipe. These deformations are the cause of non-uniformity of pipe's cross section (so-called "ovality" of pipe section).

Figures 10-12 present effective stress at the outer and inner surfaces of the pipe along helical weld path. It can be noticed that residual stress (after cooling period, $t$ = 25 s) is similar at outer and inner surface. It can be observed a slight difference between effective stresses calculated for three different models of thermal.

Figure 13 presents distribution of residual stress on the outer surface of welded pipe, for time period $t$ = 25s (this time reflects the cooling period). It can be observed that welding stress for the three welding methods are similar. Residual stress remains high along welding line, in heat source activity zone with the highest values about 240 MPa.
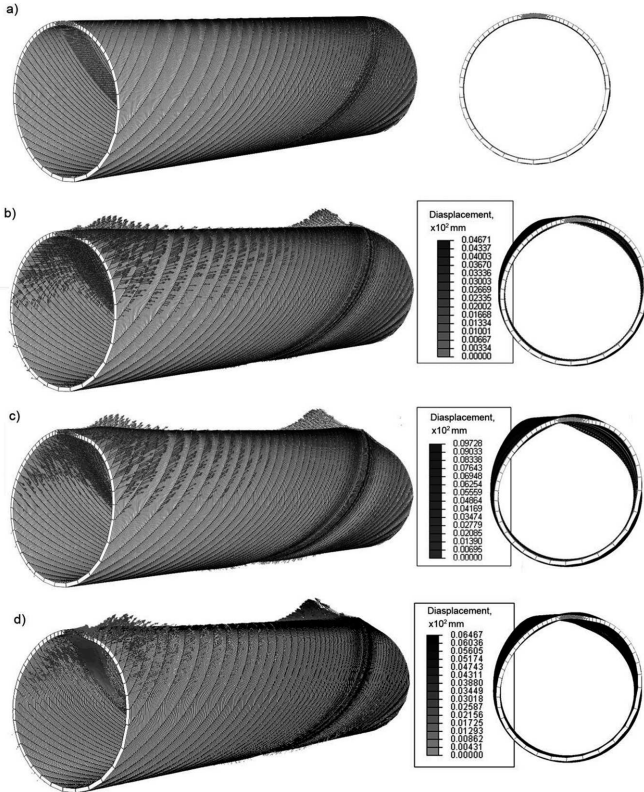


Fig. 9. Geometry of a pipe before welding a) and calculated deformations in a) laser beam welding, b) electric arc welding and c) laser-arc hybrid welding processes
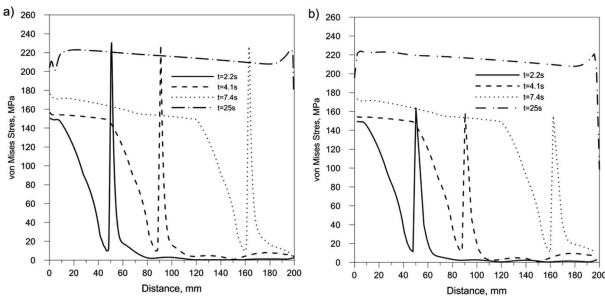


Fig. 10. Effective stress along the helical weld path at the a) outer and b) inner surfaces of laser welded pipe
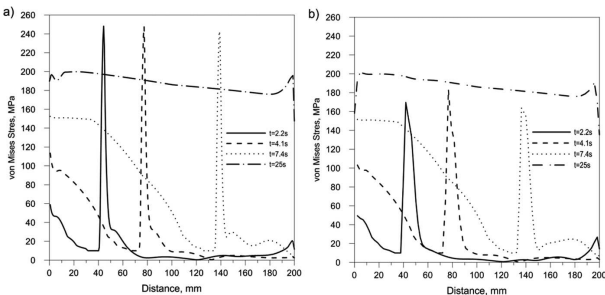


Fig. 11. Effective stress along the helical weld path at the a) outer and b) inner surfaces of arc welded pipe
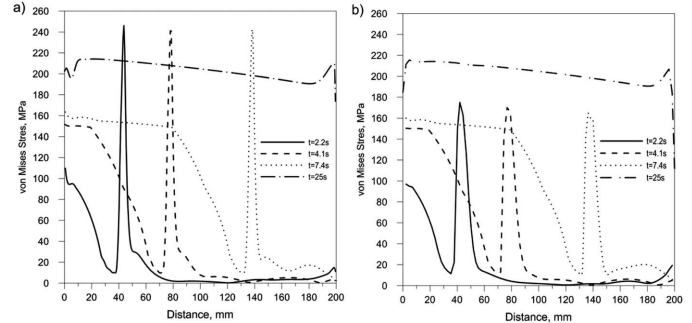


Fig. 12. Effective stress along the helical weld path at the a) outer and b) inner surfaces of laser-arc hybrid welded pipe



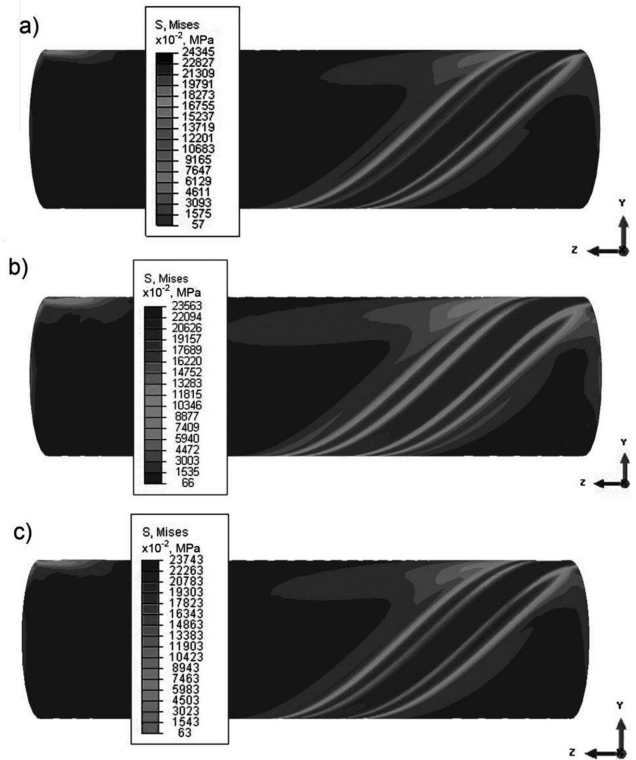Fig. 13. Residual stress distribution in simulation of a) laser beam welding, b) arc welding and c) laser-arc hybrid welding methods

## 4. Conclusions

Three dimensional transient thermomechanical analysis was performed in Abaqus FEA for spirally welded pipe made of stainless steel. Temperature field, deformations and effective stress were estimated in two steps consisted of thermal and mechanical analysis.

From calculated temperature distribution in laser beam welding (Fig. 6) it can be concluded that the laser heat source provides narrow melted zone and small thermal influence on the material, whereas in hybrid welding leading electric arc melts upper parts of the workpiece allowing the laser beam to

penetrate deeper into welded material (Fig. 8). This synergy effect of two heat sources interacting in the welding pool allows decreasing the laser beam and arc heat sources powers with simultaneous increase of welding speed.

On the basis of numerically obtained results significant differences in welding distortion is observed at similar residual stress. From the comparison estimated deformations it can be noticed that the smallest distortion and "ovality" of spirally welded pipe is achieved in laser welding process (Fig. 9). However, lower heat energy used in the hybrid welding process without the need for precise fit-up of joined edges as well as obtained slightly larger distortion in comparison with laser welded joint appears to be advantageous from a practical point of view.

Residual stress occurring along weld path at the outer surface is similar to residual stress at the inner surface of the pipe for each analyzed case. Sharp increase in effective stress in the heat source activity zone results from high temperature gradients (Fig. 10-12). Numerically estimated effective stress in laser beam welding process is smaller than obtained during hybrid welding simulation. At the outer surface of hybrid welded pipe the influence of arc heat source on effective stress distribution is noticeable (Fig. 11a and Fig. 12a), while at the inner surface effective stress results directly from the interaction of the laser beam on the material (Fig. 10b and 12b).

Developed numerical model and implemented additional subroutines allow the simulation of spirally welded pipes and estimate proper technological parameters as well as various geometrical constraints. Presented models may be helpful in prediction of welded joints quality in terms of different process parameters.

## REFERENCES

[1] Y. K o m i z o, Overview of recent welding technology relating to pipeline construction, Trans of JWRI **37**, 1-5 (2008).

[2] D. C h r o m i k, Nowoczesne technologie spawalnicze, Rurociągi **54**, 15-17 (2008).

[3] Welded Steel Pipe Design Manual. Merits, Design Standards, Technical Data and References, American Iron And Steel Institute, USA (2007).

[4] J. P i l a r c z y k, M. B a n a s i k, J. S t a n o, Technological applications of laser beam welding and cutting at the Instytut Spawalnictwa, Przeglad Spawalnictwa **5-6**, 6-10 (2006).

[5] J. R o j e k, M. H y r c z a - M i c h a l s k a, A. B o k o t a, W. P i e k a r s k a, Determination of Mechanical Properties of the Weld Zone in Tailor-Welded Blanks, Arch Civ Mech Eng **12**, 156-162 (2012).

[6] C. D a v e s, Laser Welding: A practical guide, Abington Publishing, Cambridge (1992).

[7] U. D i l t h e y, A. W i e s c h e m a n n, Prospects by combining and coupling laser beam and arc welding processes, Welding in the World **44**, 37-46 (2000).

[8] P. S e y f f a r t h, I.V. K r i v t s u n, Laser-Arc Processes and their Applications in Welding and Material Treatment, Taylor & Francis, USA (2002).

[9] A. B o k o t a, T. D o n a ń s k i, Numerical Analysis of thermo-mechanical phenomena of hardening process of elements made of carbon steel C80U, Arch Metall Mater **52**, 277-288 (2007).

[10] M.J. T o r k a m a n y, J. S a b b a g h z a d e h, M.J. H a m e - d i, Effect of laser welding mode on the microstructure and mechanical performance of dissimilar laser spot welds between low carbon and austenitic stainless steels, Mater Design **34**, 666-672 (2012).

[11] J. Z h o u, H.L. T s a i, Modeling of transport phenomena in hybrid laser–MIG keyhole welding, Int J Heat Mass Trans **51**, 4353-4366 (2008).

[12] W. P i e k a r s k a, M. K u b i a k, A. B o k o t a, Numerical simulation of thermal phenomena and phase transformations in laser-arc hybrid welded joints, Arch Metall Mater **56**, 409-421 (2011).

[13] F. Y i g i t, L.G. H e c t o r, Solidification of a pure metal with finite thermal capacitance on a sinusoidal mold surface, J Therm Stresses **25**, 663-690 (2002).

[14] M.A. R a d y, V.V. S a t y a m u r t y, A.K. M o h a n t y, Effects of liquid superheat during solidification of pure metals in a square cavity, Heat Mass Transfer **32**, 499-509 (1997).

[15] T. S k r z y p c z a k, E. W ę g r z y n - S k r z y p c z a k, Mathematical and numerical model of solidification process of pure metals, Int J Heat Mass Trans **55**, 4276-4284 (2012).

[16] E. M a j c h r z a k, B. M o c h n a c k i, J.S. S u c h y, Identification of substitute thermal capacity of solidifying alloy, J Theor Appl Mech **46**, 257-268 (2008).

[17] B. N e d j a r, An enthalpy-based finite element method for nonlinear heat problems involving phase change, Comput Struct **80**, 9-21 (2002).

[18] R. P a r k i t n y, L. S o w a, Numerical simulation of solidification of casting taking into account fluid flow and heat transfer phenomena. The axisymmetrical problem, J Theor Appl Mech **39**, 909-921 (2001).

[19] SIMULIA; Abaqus analysis user's manual. Version 6.7; Dassault System (2007).

[20] SIMULIA; Abaqus theory manual. Version 6.7; Dassault System (2007).

[21] S.A. T s i r k a s, P. P a p a n i k o s, Th. K e r m a n i d i s, Numerical simulation of the laser welding process in butt-joint specimens, J Mater Process Tech **134**, 59-69 (2003).

[22] J.A. G o l d a k, Computational Welding Mechanics, Springer, USA (2005).

[23] D. D e n g, H. M u r a k a w a, Numerical simulation of temperature field and residual stress in multi-pass welds in stainless steel pipe and comparison with experimental measurements, Comp Mater Sci **37**, 269-277 (2006).

[24] A.F.M. A r i f, A.S. A l - O m a r i, B.S. Y i l b a s, Y.N. A l - N a s s a r, Thermal stress analysis of spiral laser-welded tube, J Mater Process Tech **211**, 675-687 (2011).